

The endpoint of the rp process on accreting neutron stars

H. Schatz¹, A. Aprahamian², V. Barnard², L. Bildsten³, A. Cumming³, M. Ouellette¹, T. Rauscher⁴,
F.-K. Thielemann⁴, M. Wiescher²

¹ *Dept. of Physics and Astronomy and National Superconducting Cyclotron Laboratory, Michigan State University, East Lansing, MI 48824*

² *Dept. of Physics, University of Notre Dame, Notre Dame, IN 46556*

³ *Institute for Theoretical Physics, University of California, Santa Barbara, CA 93106*

⁴ *Dept. of Physics and Astronomy, Universität Basel, Klingelbergstr. 82, CH-4056, Basel, Switzerland*
(October 22, 2018)

We calculate the rapid proton (rp) capture process of hydrogen burning on the surface of an accreting neutron star with an updated reaction network that extends up to Xe, far beyond previous work. In both steady-state nuclear burning appropriate for rapidly accreting neutron stars (such as the magnetic polar caps of accreting X-ray pulsars) and unstable burning of Type I X-ray bursts, we find that the rp process ends in a closed SnSbTe cycle. This prevents the synthesis of elements heavier than Te and has important consequences for X-ray burst profiles, the composition of accreting neutron stars, and potentially galactic nucleosynthesis of light p nuclei.

97.80.Jp, 97.60.Jd, 26.30.+k

I. INTRODUCTION

Observations of X-ray binaries are an important source of information about neutron stars. In these systems a neutron star accretes hydrogen and helium rich matter from the envelope of a close companion star. Gravitational energy is released when the matter reaches the neutron star and powers most of the observable X-ray radiation. The accreted material is compressed, heated, and eventually undergoes thermonuclear burning. The released nuclear energy, though small relative to the gravitational energy, is observable as Type I X-ray bursts at accretion rates $\lesssim 10^{-8} M_{\odot} \text{ yr}^{-1}$. For these rates, the nuclear burning proceeds unstably [1–4], repeating on typical timescales of hours or days. In bright X-ray sources and in magnetically accreting X-ray pulsars the accretion rates reach or locally exceed the Eddington limit. The accreted layer is then thermally stable and the thermonuclear burning proceeds in steady state [5,6].

When hydrogen is present, the nuclear burning proceeds via the rapid proton capture process (rp process) [7], a sequence of proton captures and β decays responsible for the burning of hydrogen into heavier elements. We show here, for the first time, that there is a natural termination of this process due to a closed cycle in the Sn-Te region (SnSbTe cycle).

Understanding the rp process and especially its endpoint is a prerequisite for the interpretation of X-ray burst light curves, which show a wide variety of characteristics including millisecond oscillations [8]. Furthermore, the ashes of the nuclear burning replace the original crust of the neutron star and determine its thermal and electrical conductivities. The nuclear burning products thus have direct repercussions for the evolution of magnetic fields [9], the quiescent luminosity in transient X-ray binaries [10] (which could be used to discriminate against systems with accreting black holes), and the emission of potentially detectable gravitational waves from a rapidly rotating neutron star with a deformed crust [11,12]. There has also been an interest in the nuclear burning processes during X-ray bursts as a potential site for the nucleosynthesis of some light p nuclei like $^{92,94}\text{Mo}$ and $^{96,98}\text{Ru}$ that are severely underproduced in standard p process scenarios (for example [13]). This would require the escape of some of the burned material into the interstellar medium.

Many early rp process simulations for X-ray bursts were based on reaction networks that ended at ^{56}Ni . For these calculations, it was argued that further proton captures were negligible for hydrogen consumption and energy production. However, several later studies were performed with larger networks ending in the Kr-Y region [7,14–17] or using a simplified 16 nuclei network up to Cd [18]. Recently a parameter study was carried out with an updated and extended network up to Sn [19]. All of these studies found that a significant fraction of the rp process reached the end of their respective networks. An rp process reaching the end of a reaction network up to Sn was also clearly demonstrated for the steady state burning regime for accretion rates between 20 and 40 times the Eddington limit ($\dot{m}_{\text{Edd}} = 8.8 \cdot 10^4 \text{ g/cm}^2/\text{s}$) [6].

II. CALCULATIONS

In this paper we explore the rp process beyond Sn in explosive and steady state burning to determine for the first time the endpoint of the rp process. Our one-zone X-ray burst model is based on the physics outlined in reference [20]. Realistic ignition conditions have been calculated as a function of accretion rate and metallicity [21]. For the X-ray burst model we assume an accretion rate of $0.1 \dot{m}_{\text{Edd}}$, a flux out of the crust of 0.15 MeV per accreted nucleon, and a metallicity $Z = 10^{-3}$. An accreted layer with solar metallicity would produce a similar burst at a higher accretion rate of $0.3 \dot{m}_{\text{Edd}}$. The steady state model is the same as described in reference [6]. For all models we assume accretion of hydrogen and helium in solar proportions, and a surface gravity of $1.9 \times 10^{14} \text{cm/s}^2$.

The nuclear reaction network includes all proton rich nuclei from hydrogen to xenon and was updated relative to the data described in [19]. The theoretical Hauser-Feshbach reaction rates have been recalculated with the new Hauser-Feshbach code NON-SMOKER [22]. A more detailed discussion of the nuclear physics input and the X-ray burst model will be published in a forthcoming paper.

III. RESULTS

Figure 1 shows our results for the time integrated reaction flow during an X-ray burst. Ignition takes place at a density of $1.1 \times 10^6 \text{g/cm}^3$ and the burst reaches a peak temperature of 1.9 GK, with a rise time scale of ≈ 4 s, and a cooling phase lasting ≈ 200 s. Helium burns via the 3α reaction, and the αp process [7], a sequence of alternating (α, p) and (p, γ) reactions into the Sc region. These helium burning processes provide the seed nuclei for the rp process. The rp process reaction flow reaches the Sn isotopes in the ^{99}Sn - ^{101}Sn range ≈ 80 s (time for half maximum) after the burst peak and proceeds then along the Sn isotopic chain towards more stable nuclei.

Processing beyond Sn occurs if the corresponding Sb isotone is sufficiently proton bound for the (γ, p) photodisintegration to be small. This occurs at ^{105}Sn . However, after two proton captures a strong $^{107}\text{Te}(\gamma, \alpha)$ photodisintegration rate cycles the reaction flow back to ^{103}Sn . The reaction path is characterized by a cyclic flow pattern, the SnSbTe cycle which represents the endpoint for the rp-process reaction flow towards higher masses (see figure 2). The SnSbTe cycle forms because the neutron deficient $^{106-108}\text{Te}$ isotopes are α unbound by ≈ 4 MeV. In fact, ^{107}Te is a known ground state α emitter [23]. A fraction of the reaction flow proceeds via β decay of ^{105}Sn into ^{106}Sn , and the reaction sequence $^{106}\text{Sn}(p, \gamma)^{107}\text{Sb}(p, \gamma)^{108}\text{Te}(\gamma, \alpha)^{104}\text{Sn}$ leads to a second, weaker cycle. Calculations with different ignition conditions confirm that the rp process cannot proceed beyond the SnSbTe cycles.

A previous calculation of the rp process in steady state burning found that most material accumulated at the end of the network (the Sn isotopes) for an accretion rate of $40\dot{m}_{\text{Edd}}$ [6]. Figure 1 shows the reaction flow at that accretion rate. We find that the rp process ends in a similar SnSbTe cycle as in X-ray bursts. Some of the material is now cycled back via $^{106}\text{Sb}(p, \alpha)$, which successfully competes with $^{106}\text{Sb}(p, \gamma)$ at steady state burning conditions. Calculations at different accretion rates show that the rp process can never overcome the closed SnSbTe cycle. For steady state burning, we are now able to compute accurately the composition of the ashes for all accretion rates.

The SnSbTe cycle impacts the light-curve of X-ray bursts and the consumption of hydrogen. This is illustrated in figure 3, which shows the correlation between the X-ray burst luminosity, the abundances of some important long lived nuclei (waiting points) in the rp process, and the hydrogen and helium abundances. Clearly the slow hydrogen burning via the rp process beyond ^{56}Ni is responsible for the extended burst tail. The SnSbTe cycle builds up the abundance of the longest lived nucleus in the cycle, ^{104}Sn (20.8 s half-life), and produces helium towards the end of the burst. This triggers an increase in the 3α flow and subsequently an increase in energy production and hydrogen consumption. As a consequence, the burst lasts longer and hydrogen is completely burned.

The SnSbTe cycle also affects the composition of the rp process ashes, shown for the X-ray burst and the steady state calculation in figure 4. The limitation imposed on the rp process by the SnSbTe cycle is clearly reflected in the lack of nuclei heavier than $A = 107$. Nevertheless we obtain a broad distribution of nuclei in the $A = 64$ -107 mass range. This is a result of the long lived waiting point nuclei along the rp process reaction path which store some material until the burning is over. The late helium production in the SnSbTe cycle broadens this distribution further.

IV. CONCLUSIONS

To summarize, we have shown that the synthesis of heavy nuclei via the rp process is limited to nuclei with $Z \leq 54$ due to our newly discovered SnSbTe cycle. The existence of a SnSbTe cycle under all rp process conditions is a consequence of the low, experimentally known [24] α separation energies of the $^{106,107,108,109}\text{Te}$ isotopes and is therefore not subject to nuclear physics uncertainties. However, because of the uncertainties in the proton separation

energies of the Sb isotopes there is some uncertainty in the relative strength of the SnSbTe sub-cycles closed by (γ, α) photodisintegration on ^{106}Te , ^{107}Te , and ^{108}Te . This will be discussed in a forthcoming paper.

A likely consequence of the SnSbTe cycle for accreting neutron stars is that the matter entering the crust is composed of nuclei lighter than $A \approx 107$. The only way to bypass the SnSbTe cycle would be a pulsed rp process, where between pulses matter could decay back to stable nuclei. This could happen during so called dwarf bursts, which have been suggested to be secondary bursts produced by reignition of the ashes [25]. However, this would require some unburned hydrogen in the burst ashes (see discussion below) or extensive vertical mixing [14].

Our calculations give a strong indication that the synthesis of nuclei beyond ^{56}Ni and especially into the $A = 100$ mass region in hydrogen rich bursts leads to extended energy production. This might explain the long duration (100 seconds) bursts seen from, for example, GS 1826-24 [26].

The importance of the endpoint of the rp process for the consumption of hydrogen in X-ray bursts has been discussed extensively. Previous calculations limited to nuclei up to ^{56}Ni always found unburned hydrogen. Later burning of this hydrogen was proposed to explain short burst intervals [25], occasionally observed extended X-ray flares [27], and spin down in millisecond oscillations, as recently discovered during the tail of a long X-ray burst from 4U 1636-53 [28]. It was pointed out before that depending on the endpoint of the rp process these models might largely overestimate the amount of unburned hydrogen [14]. Our calculations indicate indeed that the SnSbTe cycle reduces the amount of unburned hydrogen substantially. Within the framework of the one-zone model we find that all the hydrogen is burned, a full multizone hydrodynamic burst calculation is needed to confirm this result.

In our X-ray burst calculation, we find large overproduction factors (produced abundance to solar abundance $\approx 10^9$) for the p nuclei ^{98}Ru , ^{102}Pd , and ^{106}Cd . Overproduction factors of this order have been suggested to be sufficient to explain the origin of the solar system abundances of these nuclei if $\approx 1\%$ of the burned material is somehow ejected [19]. However, in order to accurately calculate the composition of the ejected material the ejection mechanism has to be identified. Furthermore we find that the synthesis of p nuclei is most likely associated with X-ray bursts having long tails. As these bursts are rare, we conclude that only a small fraction of X-ray bursts are likely to produce light p nuclei in the $A = 90 - 106$ mass range. Therefore, considerably larger amounts of matter would have to be ejected in X-ray bursts to account for the galactic abundances of light p nuclei than previously assumed. Nevertheless it is striking that the SnSbTe cycle happens to naturally limit rp process nucleosynthesis to light p nuclei.

The authors would like to thank R. Boyd and E. Roeckl for helpful discussions. Part of this work was carried out under NSF contract PHY-95-28844, PHY-99-01133 and PHY-99-07949, under NASA grant NAG5-8658, and under and the Swiss NSF contracts 2124-055832.98 and 2000-061822.00. L.B. is a Cottrell Scholar of the Research Corporation. V.B. was supported through the Graduate School of the University of Notre Dame.

-
- [1] S. E. Woosley and R. E. Taam, *Nature* **263**, 101 (1976).
 - [2] L. Maraschi and A. Cavaliere, *Highlights of Astronomy* **4**, 127 (1977).
 - [3] P. C. Joss, *Nature* **270**, 310 (1977).
 - [4] W. H. G. Lewin, J. van Paradijs, and R. E. Taam, in *X-Ray Binaries*, edited by W. H. G. Lewin, J. van Paradijs, and E. P. J. van den Heuvel (Cambridge Univ. Press, Cambridge) p. 175
 - [5] P. C. Joss and F. K. Li, *Ap. J.* **238**, 287 (1980).
 - [6] H. Schatz, L. Bildsten, A. Cumming, and M. Wiescher, *Ap. J.* **524**, 1014 (1999).
 - [7] R. K. Wallace and S. E. Woosley, *Ap. J. Suppl.* **45**, 389 (1981).
 - [8] T. Strohmayer, J. Swank, and W. Zhang, *Nucl. Phys. B (Proc. Suppl.)* **69**, 129 (1998).
 - [9] E. F. Brown and L. Bildsten, *Ap. J.* **496**, 915 (1998).
 - [10] E. F. Brown, L. Bildsten, and R. E. Rutledge, *Ap. J.* **504**, L95 (1998).
 - [11] L. Bildsten, *Ap. J.* **501**, L89 (1998).
 - [12] G. Ushomirsky, L. Bildsten, and C. Cutler, *Mon. Not. Roy. Astr. Soc.*, **319**, 902 (2000)
 - [13] M. Rayet *et al.*, *Astron. Astrophys.* **298**, 517 (1995).
 - [14] M. Y. Fujimoto, M. Sztajno, W. H. G. Lewin, and J. van Paradijs, *Ap. J.* **319**, 902 (1987).
 - [15] T. Hanawa, D. Sugimoto, and M.-A. Hashimoto, *Pub. Astr. Soc. Japan* **35**, 491 (1983).
 - [16] L. Van Wormer *et al.*, *Ap. J.* **432**, 326 (1994).
 - [17] O. Koike, M. Hashimoto, K. Arai, and S. Wanajo, *Astron. Astrophys.* **342**, 464 (1999).
 - [18] R. K. Wallace and S. E. Woosley, in *High Energy Transients in Astrophysics*, Vol. 115 of *AIP Conference Proceedings*, edited by S. E. Woosley (American Institute of Physics, New York, 1984), p. 319.
 - [19] H. Schatz *et al.*, *Phys. Rep.* **294**, 167 (1998).

- [20] L. Bildsten, in *The Many Faces of Neutron Stars*, edited by R. Buccheri, J. van Paradijs, and M. A. Alpar (Dordrecht, Kluwer, 1998), p. 419
- [21] A. Cumming and L. Bildsten, *Ap. J.* **544** 453 (2000)
- [22] T. Rauscher and F.-K. Thielemann, *At. Data Nucl. Data Tab.* **75**, 1 (2000).
- [23] D. Schardt *et al.*, *Nucl. Phys. A* **326**, 65 (1979).
- [24] R. Page *et al.*, *Phys. Rev. C* **49**, 3312 (1994).
- [25] R. E. Taam, S. E. Woosley, T. A. Weaver, and D. Q. Lamb, *Ap. J.* **413**, 324 (1993).
- [26] A. Kong *et al.*, *Mon. Not. Roy. Astr. Soc.* **311**, 405 (2000).
- [27] R. E. Taam, S. E. Woosley, and D. Q. Lamb, *Ap. J.* **459**, 271 (1996).
- [28] T. Strohmayer, *Ap. J.* **523**, L51 (1999).

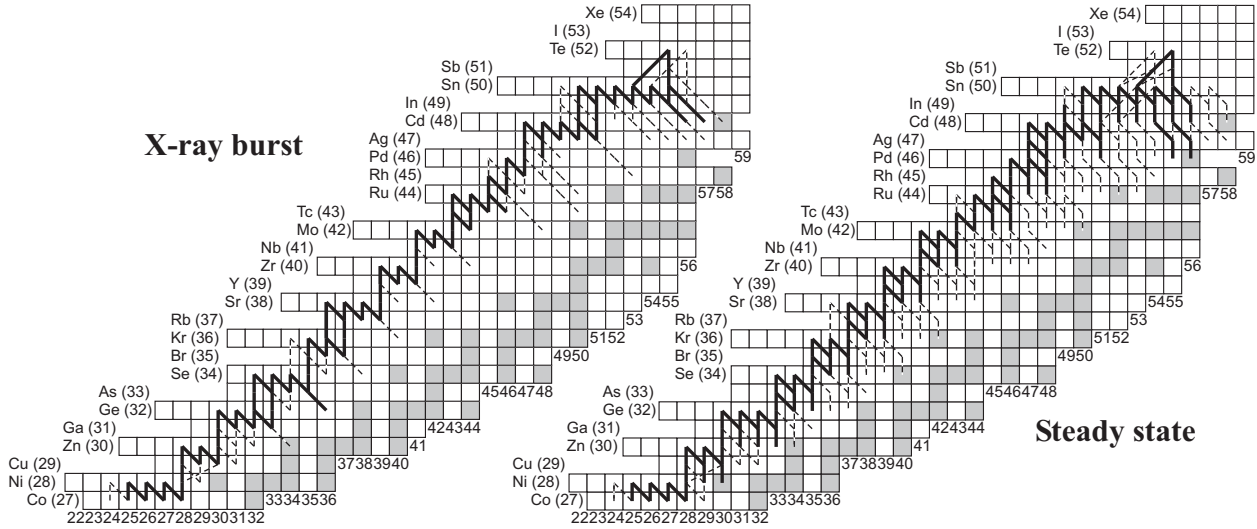


FIG. 1. The time integrated reaction flow above Ga during an X-ray burst and for steady state burning. Shown are reaction flows of more than 10% (solid line) and of 1-10% (dashed line) of the reaction flow through the 3α reaction.

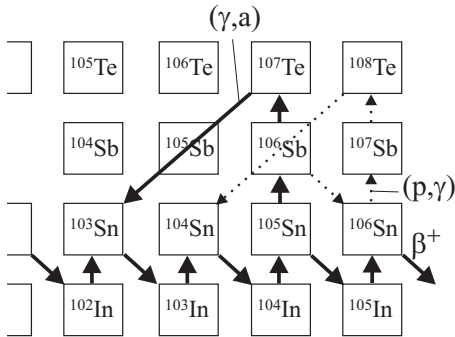


FIG. 2. The reactions in the SnSbTe cycles during an X-ray burst. In the case of proton captures the arrows indicate the direction of the net flow, the difference of the flow via proton capture and the reverse flow via (γ, p) photodisintegration. The line styles are the same as in figure 1.

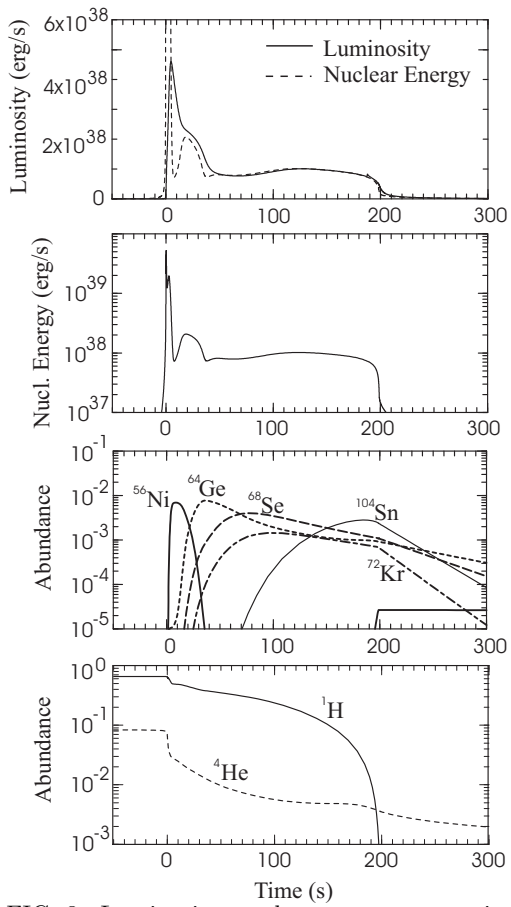


FIG. 3. Luminosity, nuclear energy generation rate, and the abundances of hydrogen, helium and the important waiting point nuclei as functions of time during an X-ray burst. For comparison, the nuclear energy generation rate is also shown as a dashed line together with the luminosity, though it is out of scale during the peak of the burst. The mass of the accreted layer is 4.9×10^{21} g.

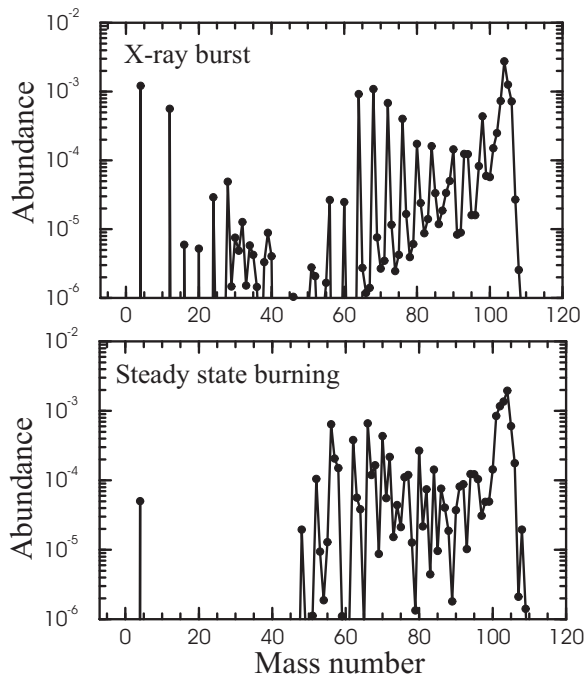


FIG. 4. Final abundance distribution as functions of mass number for an X-ray burst, and for steady state burning at an accretion rate of $40\dot{m}_{\text{Edd}}$.